Overview of SST-1 Up-gradation and Recent Experiments in SST-1

S. Pradhan, Z. Khan, V. L. Tanna, U. Prasad, Y. Paravastu, D. C. Raval, H. Masand, Aveg Kumar, J. R. Dhongde, S. Jana, B. Kakati, K. B. Patel, M. K. Bhandarkar, B. K. Shukla, D. Ghosh, H. S. Patel, T. J. Parekh, I. A. Mansuri, K. R. Dhanani, A. Varadharajulu, Y. S. Khristi, P. Biswas, C. N. Gupta, S. George, P. Semwal, D. K. Sharma, H. K. Gulati, K. Mahajan, B. R. Praghi, M. Banaudha, A. R. Makwana, H. H. Chudasma, M. Kumar, R. Manchanda, Y. S. Joisa, K. Asudani, S. N. Pandya, S. K. Pathak, S. Banerjee, P. J. Patel, P. Santra, F. S. Pathan, P. K. Chauhan, M. S. Khan, P. L. Thankey, A. Parkash A, P. N. Panchal, R. N. Panchal, R. J. Patel, G. I. Mahsuria, D. P. Sonara, K. M. Patel, S. P. Jayaswal, M. Sharma, J. C. Patel, P. Varmora, G. L. N. Srikanth, D. R. Christian, A. Garg, N. Bairagi, G. R. Babu, A. G. Panchal, M. M. Vora, A. K. Singh, R. Sharma, H. D. Nimavat, P. R. Shah, G. Purwar, T. Y. Raval, A. L. Sharma, A. Ojha, S. Kumar, N. K. Ramaiya, V. Siju, M. V. Gopalakrishna, A. Kumar, P. K. Sharma, P. K. Atrey, S.V. Kulkarni, K. K. Ambulkar, P. R. Parmar, A. L. Thakur, J. V. Raval, S. Purohit, P. K. Mishra, A. N. Adhiya, U. C. Nagora, J. Thomas, V. K. Chaudhari, K. G. Patel, S. Dalakoti, C. G. Virani, S. Gupta, Ajay Kumar, B. Chaudhari, R. Kaur, R. Srinivasan, A. N. Sharma, K. J. Doshi, D. Raju, D. H. Kanabar, R. Jha, A. Das, D. Bora & SST-1 Team

Institute for Plasma Research, Bhat Village, Gandhinagar-382 428, India

E-mail contact of main author: pradhan@ipr.res.in

Abstract. Steady State Superconducting Tokamak (SST-1) is a `working' experimental superconducting device since late 2013. Referring to the last IAEA-FEC; SST-1 has been upgraded with Plasma Facing Components (PFC) with an objective towards long pulse operations in both circular and elongated configurations. The PFC integration has been completed in August 2015 and initial experiments have begun in SST-1 with circular plasma configurations. SST-1 offers a unique possibility of investigating long pulse discharges with large aspect ratio (> 5.5) compared to contemporary devices. Presently, SST-1 standard Ohmic discharges are in excess of 100 kA with typical core density ~ 1×10^{19} m^{-3} and core electron temperatures ~ 200-300 eV having duration in excess of 300 ms. A 42 GHz ECR pre-ionization source at ~ 150 kW in 1.5 T central toroidal field breaks down the hydrogen gas, the current starts up at ~ 1.3 MA/s in 60-80 ms in an induced electric field of ~ 0.3 V/m. These standard discharges demonstrate copious saw teething and MHD activities as the pulse progresses including NTM, mode locking and MHD characteristics. Studies on eddy currents influencing the NULL dynamics, field errors, equilibrium index evolutions, wall influencing plasma characteristics, plasma positions, plasma rotational andTearing Mode characteristics including the island width and growth etc. have been carried out. Presently, SST-1 is attempting at multi-second long high aspect ratio plasma discharges by coupling the Lower Hybrid with the Ohmic plasma as well as with robust real time position and density controls. SST-1 device has also been upgraded with a pair of internal coil aimed at effective fast plasma control and a pair of segmented coil aimed at controlling some of the rotational aspects of plasma including the RMPs and ELMs. Supersonic Molecular Beam Injection (SMBI) from both high field and low field sides and Pellets Injection Systems have also been added with several edge plasma diagnostics aimed at both density control and edge plasma turbulence studies. This paper elaborates some of these up-gradation and results from the initial experiments.

1. Introduction

Steady State Superconducting Tokamak (SST-1) is a `working' experimental superconducting device since late 2013. In the long term, SST-1 envisages steady state operation in both the single null and double null configurations in large aspect ratio configurations [1]. The primary magnetic configurations and plasma shaping magnetic requirements are provided by Superconducting Magnet Systems (SCMS) comprising of sixteen superconducting D-shaped Toroidal Field (TF) magnets and nine superconducting Poloidal Field (PF) magnets together with a pair of resistive PF coils inside the vacuum vessel. An air core Ohmic transformer together with three pairs of resistive compensating coils together with a 500 kW, 500 ms Gyrotron are used for the pre-ionization, initial break-down and initial current start-up. A pair of resistive vertical field magnets outside the cryostat placed symmetrically around the mid plane provides the initial equilibrium. Fig.1 shows various components of SST-1 machine shell.

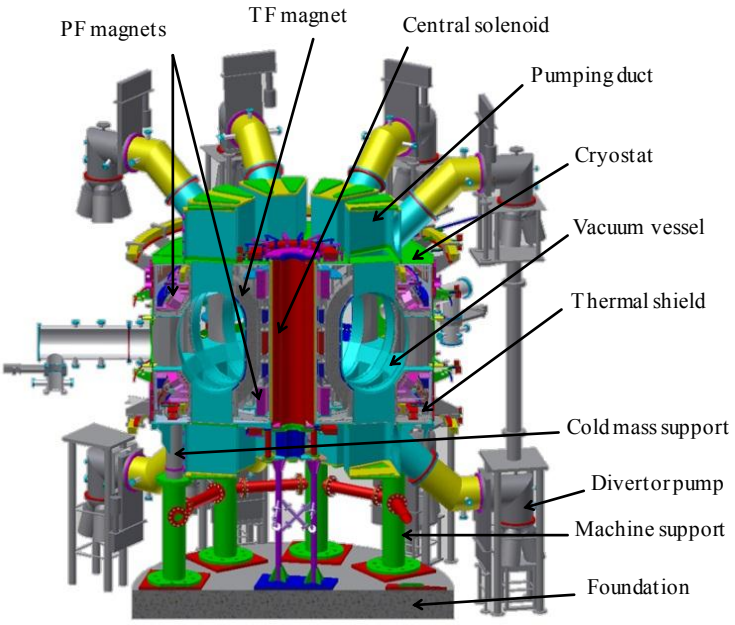

FIG. 1.3D cut view of SST-1 Machine

TABLE I Major SST-1 machine parameters (PFC related)

Parameters	Values
Major radius	1.1 m
Minor radius	0.2 m
SS surface area of VV	75 m^2
Exposed surface area of PFC	40 m^2
Plasma species	Hydrogen
Volume enclosed by PFC	16 m^3
Steady State Heat Flux	
Main Baffle	0.25 MW/m^2
In / Outboard Passive Stabilizer	0.25 MW/m^2
In / Outboard Divertor Plate	0.6 MW/m^2
In / Outboard Poloidal Limiter	1.0 MW/m^2

After obtaining a plasma current of ~75 kA at a central field of 1.5 T for ~500 ms in a limiter equipped SST-1in 2014, as part of phase-1 up-gradation of SST-1Plasma Facing Components (PFC) were installed successfully during Oct 2014-May 2015 (Table-1). Subsequently, PFC equipped SST-1 underwent a rigorous 'engineering validation' to validate leak tightness, thermal and electrical isolations, meteorology consistencies etc.described in section 2 of this paper. Initial experiments also quantified eddy currents influencing the NULL, the plasma break-down and start-ups, the equilibrium field index and the initial equilibrium etc. in the PFC equipped SST-1 as described in section-3 of the paper. The MHD aspects, Disruption, Edge Turbulence and Radial transport observed have been elaborated in section-4. The future plans inclusive of engineering up-gradation and physics on SST-1 have been briefly outlined in section 5 of this paper along with a summary.

2. SST-1 Up-gradation (Phase-1)

During 2014-15, major up-gradation in SST-1 has been carried out involving PFC integration and cryogenic flow distribution and control (IFDC) system.

2.1. PFC Up-gradation

SST-1 Tokamak was successfully commissioned in 2012 and the first plasma was obtained in June 2013 with poloidal limiters, and having SS 304L as vessel wall material. In the phase-1 up-gradation [2], Graphite based PFCs designed to withstand an input heat load of 1.0 MW/m^2 have been mounted on a back plate made of Cu-Zr & Cu-Cr-Zr alloys embedded with SS 304L piping to carry the heat away. Approximately 3800 tiles have been mounted on 132 numbers of copper alloys back-plates on a surface area of 40 m^2 on a vacuum vessel volume of ~ 16 m^3. PFC components are baked up to 250°C in steady state under UHV conditions with a hot nitrogen baking system while keeping the vacuum vessel at 150°C.

A combination of ECDS and Photogrammetric measurements (Fig.2) has ensured the assembly of the PFC components. The assembled PFC with their support structures are shown in Fig. 3 & Fig. 4.

FIG. 2. Coded and un-coded targets mounted on prototype vacuum vessel and co-ordinate generation in AUSTRALIS 7.0 software.

FIG. 3.Full assembly of copper module in SST-1 vessel

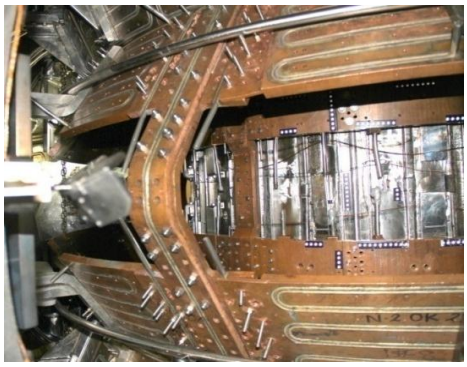

FIG. 4. Final assembly of PFC modules in SST-1 vessel

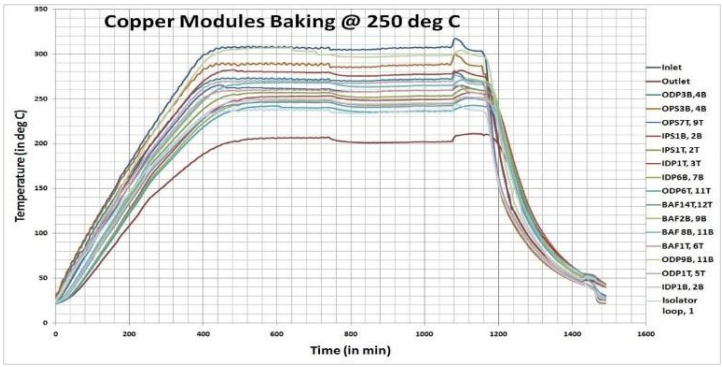

FIG. 5: Performance of Baking of Copper Modules at 250°C

Graphite tiles are mechanically bolted on the back plate with a graphoil sheet in between to ensure good thermal contact whereas the temperature of the back plate is monitored with thermocouples. As a part of PFC conditioning, a baking of the components is carried out at 250°C for extended duration (Fig. 5). After words, prior to plasma experiments hydrogen discharge cleaning followed by extended helium discharge cleaning are usually carried out.

2.2. IFDC Up-gradation

Hydraulic imbalances and thermal run way had been observed amongst the different hydraulic path lengths of the PF coils systems. The original PF distribution scheme had a single control valve for the entire PF magnets. The flow distribution scheme has been subsequently modified (Fig. 6 and 7) balancing the hydraulic impedances to various unequal PF flow paths. With these modifications and up-gradations, the cooling down in PF magnets have now been devoid of thermal run away.

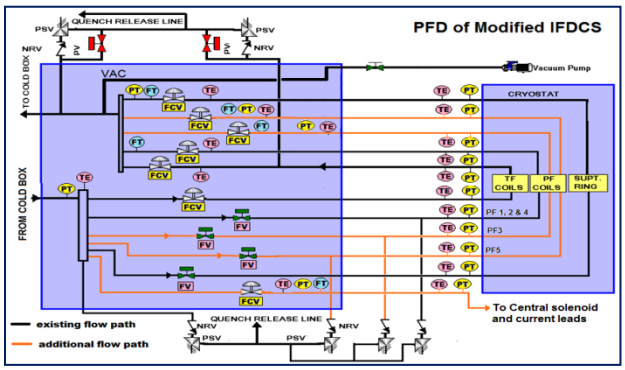

FIG.6: Process flow and instrumentation diagram of upgraded IFDCS

FIG.7: Snapshots of Installation of upgraded IFDCS and 3S-2R transfer line

3. Initial validations of the PFC equipped SST-1 circular plasma

3.1. Eddy current Aspects and Equilibrium Re-construction

Eddy currents temporal and spatial characteristics have altered in the PFC equipped SST-1 compared to the earlier limiter equipped SST-1 and thereby was influencing the transient field errors and subsequently the magnetic NULL and break-down characteristics. A detailed quantitative distribution of the eddy current in the electrically continuous SST-1 vacuum vessel have been computed employing the array of internal voltage loops (flux loop) and with the help of simple circuit model [3, 4].The computed results from this model have been benchmarked against experimental measured integrated eddy current. The computed values and the experimentally measured values are in good agreement, in general including their temporal behaviour.

Both the rate of change of current in the central solenoid (dI_{OT}/dt) as well as the sudden disappearance of plasma current during a disruption leading to forces acting on the vacuum vessel of SST-1 have been analysed in detail. The calculated eddy current based on flux loop signal and circuit equation model have been extended towards the reconstruction of the vessel magnetic field line (B-field) for SST-1. Comparison between the field line of plasma and vacuum shot explains the plasma current contribution from all other sources also.

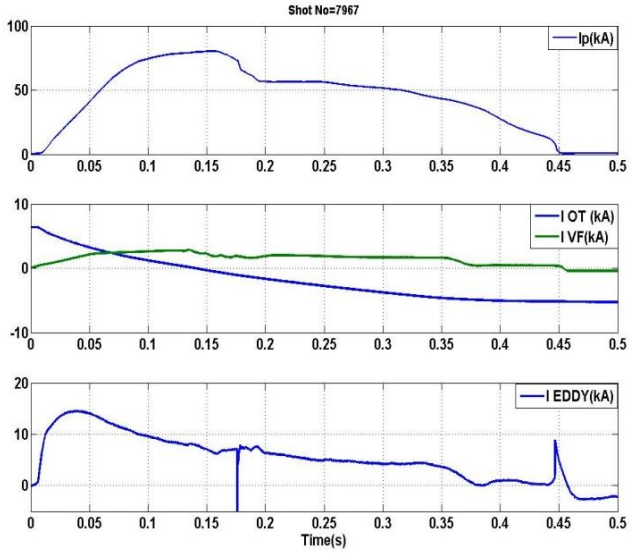

FIG. 8. Total eddy current with IP=0 and IOT, IVF (green) for plasma shot no 7967

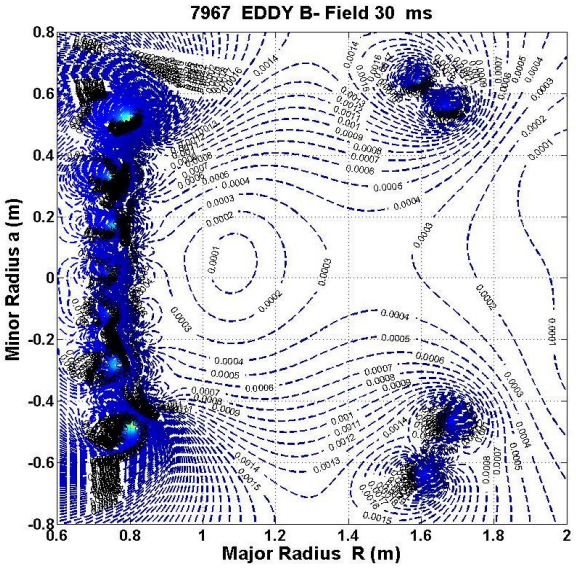

FIG. 9.The eddy B-field line of plasma shot 7967

The eddy current(Fig. 8.) and magnetic field (Fig. 9.) for eddy has been computed through a MATLAB code using simulated data calculated from each vessel sectional current and location of the segment and cryostat position. The inductance and resistive effect of vessel segments have also been included here.Results shows under representative conditions, the maximum Eddy current has been computed to be ~ 15kA.The rate of change of current in the central solenoid ($(\boldsymbol{dI}_{OT})/\boldsymbol{dt}$) and the sudden disappearance of plasma current during the disruptions are the primary sources of eddy currents apart from sudden plasma movements. The computed eddy current distributions including their temporal behaviour shall be extended to plasma equilibrium and electromagnetic modelling [5] as well as plasma discharge process in future.

3.2. Magnetic flux surfaces and Radial Shafranov shifts in SST-1 Tokamak Plasma

Magnetic flux surface contours of SST-1 tokamak [6] plasma have been computed from the magnetic probes, flux loops experimental data and from the analytical solution) [7] of Grad-Shafranov equation (GSE). SST-1 plasma, at the present phases of operations is circular in shape and leans against the limiters. The radial Shafranov shifts (ΔR) [8] from the above formulations have been calculated from experimental measurements. Since the control of plasma position plays an important role in plasma confinement and optimized tokamak operations, this ΔR would be used as a plasma position feedback control parameter in long duration SST-1 plasma experiments later. The plasma flux surface contours computed (Fig. 11) as above have also been approximately compared with the time synchronized fast imaging signals of the SST-1 plasma. These comparisons shows a good agreement between

the real time trends of plasma position shift at the equilibrium regions with those seen with fast imaging.

In Fig. 10, the plasma current and applied vertical field current (I_{VF}) have been plotted at top and bottom plot. The Radial Shafranov shift (ΔR) has been measured [9, 10] using the described flux loops and magnetic probes.

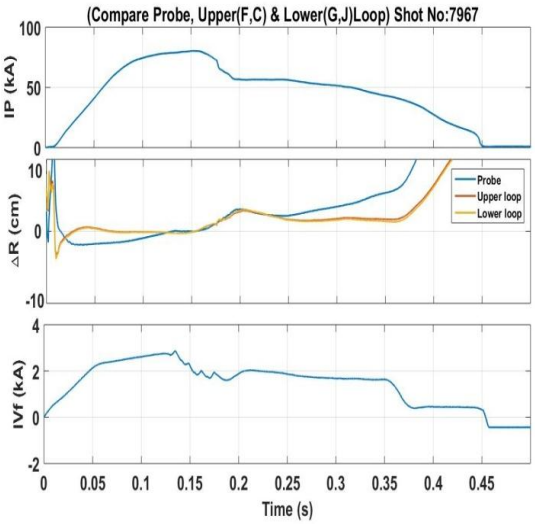

FIG.10.Plasma current (I_P), Plasma Radial shift (ΔR), $_{Plasma}$ Vertical shift (ΔZ) and Vertical Field current (I_{VF}) for SST-1 Shot No: 7967.

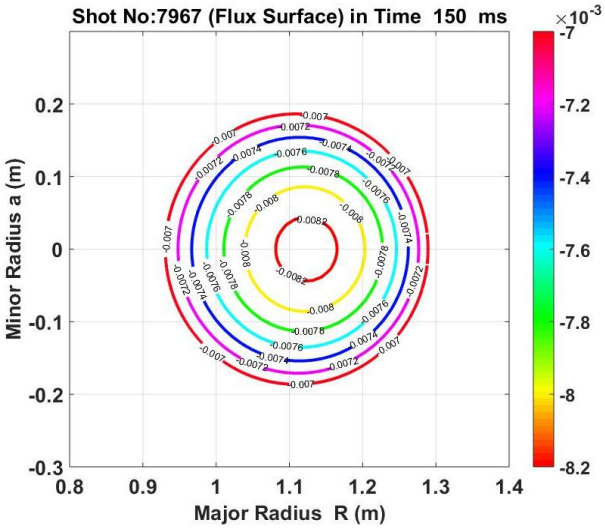

FIG. 11.Magnetic flux surface for SST-1 shot no 7967 at time instant 150ms at maximum plasma current (I_P).

The flux surface contours computed following these prescriptions have been in good agreement with the experimental data from a large number of SST-1 plasma shots. The radial Shafranov shift measured using the flux loops and magnetic probes are also in good agreement, repeatable and reliable.

3.3. Experimental Observations on Plasma Density, Temperature, Imaging

Temporal evolution of a typical SST-1 discharge (90 KA for 270 ms) is shown in Fig.11. The microwave interferometer measured line average density, n_e in this discharge is ~ 7×10^{18} m^{-3} and electron temperature, T_e is ~ 230 eV as measured from the soft X-ray diagnostics [Fig.12]. H_α signal shows a sharp breakdown peak and then settles to constant lower value throughout the plasma duration except another peak at the time of plasma termination. The radiation loss, P_{rad}, is mostly followed the n_e up to 235 ms of the discharge and rises to a peak value of 64 kW at 160 ms, which is nearly 40% of the input power. As illustrated in Fig.12e the impurity emissions signals C III at 464.7 nm and O II at 441.9 nm, also shows almost similar tends of P_{rad} except during the fag end of the discharge, when plasma wall interaction increases resulting a rising trend.

Another typical SST-1 plasma shot as shown in Fig. 12 and 13 has n_e and T_e ~ 1×10^{-19} m^{-3} and 230 eV, respectively.. However, a sharp spike in P_{rad}, H_α, O II and C III at around 204 ms is seen indicating possible higher particle influx into the plasma. Fast visible imaging (Fig. 14) shows plasma interacting with limiter in and there after regaining before terminating at 275 ms.

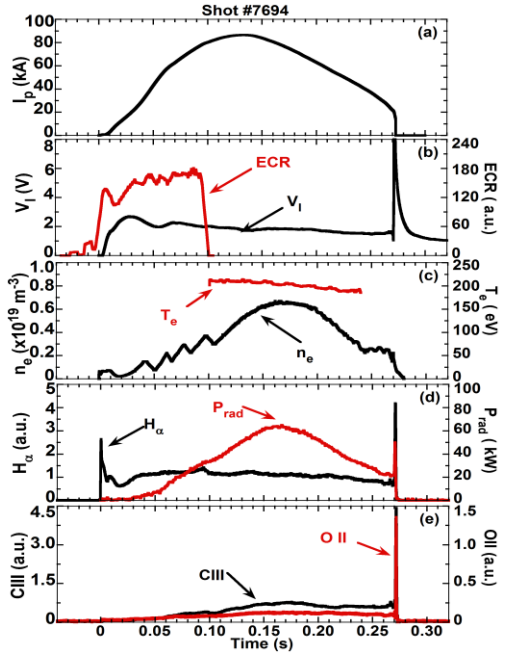

FIG. 12.Plasma Parameters in Shot #7694

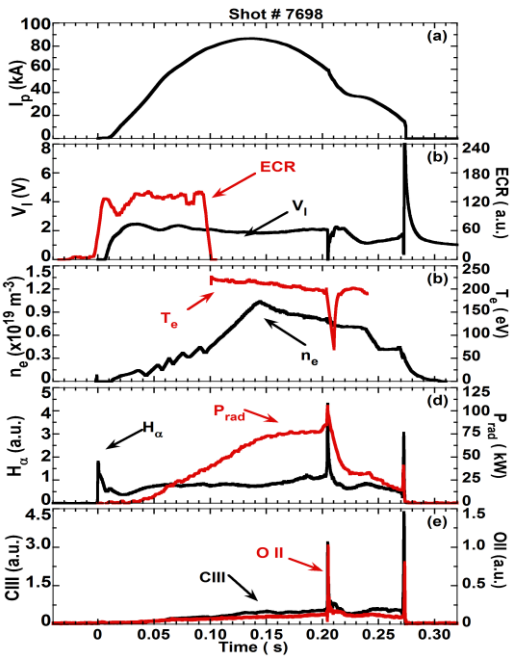

FIG. 13. Plasma Parameters in Shot

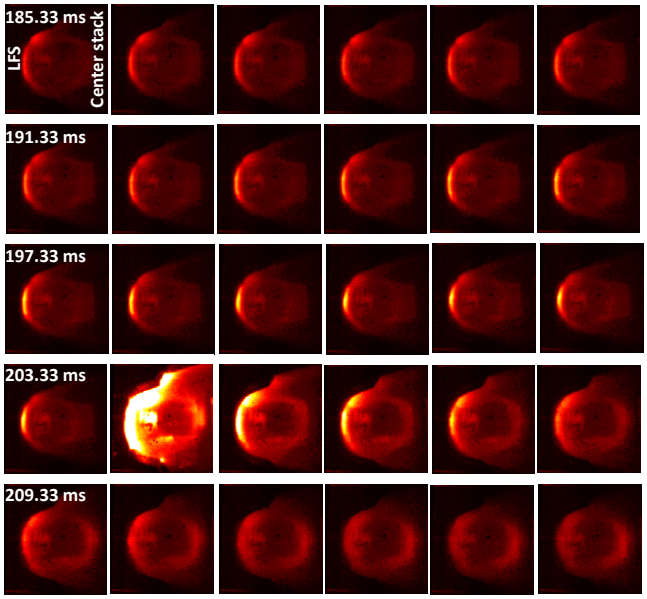

FIG. 14. Shot # 7698: Fast images acquired from a tangential line of sight at 3 kHz rate and shown at every ms. Gradual shift of the plasma column towards the low field side (LFS) and subsequent enhanced interaction with the LFS limiter can be seen at ~204.33 ms. Plasma column regains the full permissible column width thereafter. Images run left to right and top to bottom.

3.4. Higher plasma current in SST-1

With the help of a pair of radial control coil, plasma currents up to 117.55 KA have been obtained repeatedly at a central field of 1.5 T corresponding to q_{edge}~ 2.55 (Fig. 15).

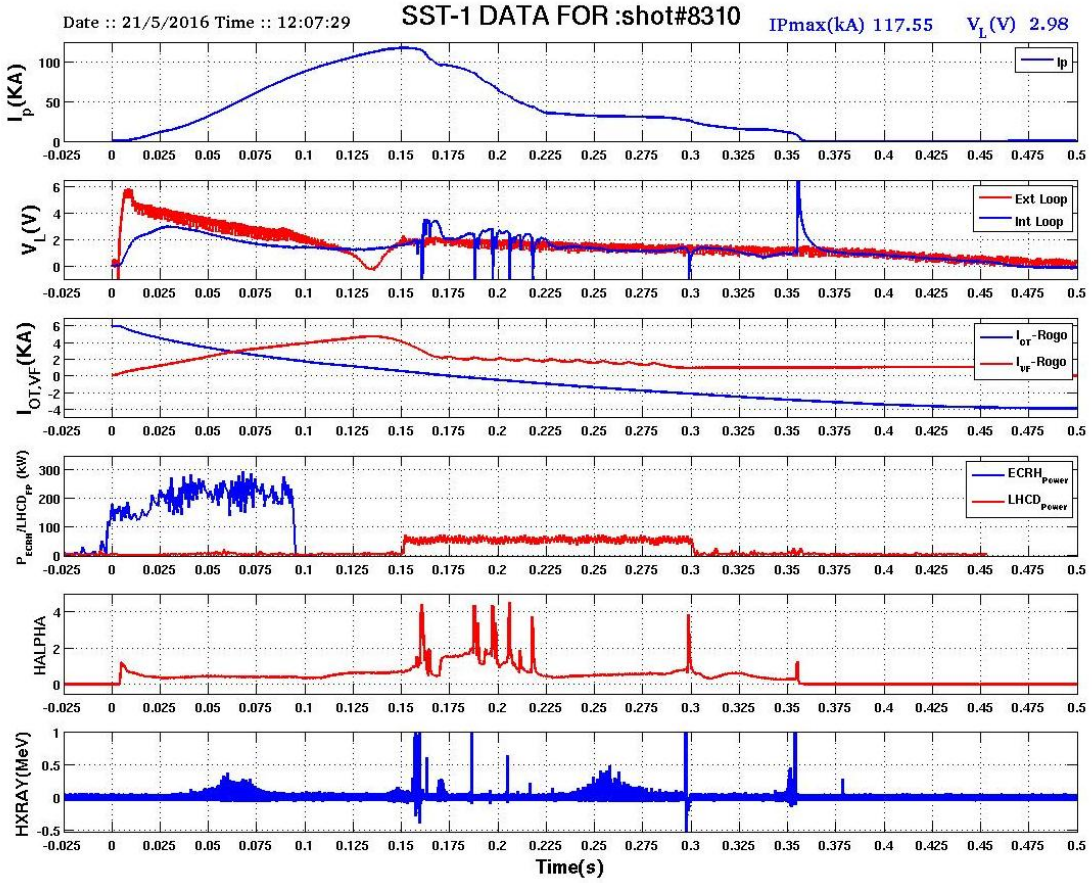

FIG.15. SST-1 shot no. 8310, (a) Plasma current, (b) Internal & External loop voltage, (c) Ohmic & Vertical field current (d) ECRH & LHCD Power, (e) Hα (f) Typical Hard X-ray signal

4. Physical findings from PFC equipped SST-1

4.1. MHD Aspects

During evolution of plasma currents (Ip) in SST-1 experiments, SST-1 came across different phenomena of magneto hydrodynamic (MHD) instabilities [11, 12, 13]. MHD phenomena observed in SST-1 experiments are at the values of edge safety factor $2.4 \leq q_a \leq 4$. Similar phenomena are also reported in other tokamaks. Earlier works [12, 13] in SST-1 mention MHD characteristics (mode frequency, mode number, island width, growth rate etc.), different MHD regimes, mode evolutions and correlation of observation with other tokamaks.

SST-1 plasma experiment with a representative shot#7607 is shown in Fig.16. The main parameters for this shot are B_T ~ 1.5T, Ip ~ 102 kA, ECRH power ~190 kW, vessel pressure (H_2) ~ $8x10^{-6}$ mbar and loop voltage ~ 2.4 V. During interval 150-160ms, the dominant frequency of Mirnov oscillations associated with tearing mode is ~ 5.9 kHz with its harmonics as shown in Fig.17. Spatial analysis using SVD method during interval 155-156.5ms reveals m=2 island structure as dominant one as shown in polar plot of Fig. 18(a). Fig. 18(b) shows the corresponding time vector i.e. oscillations resulting from rotation of spatial structure of m=2 mode.

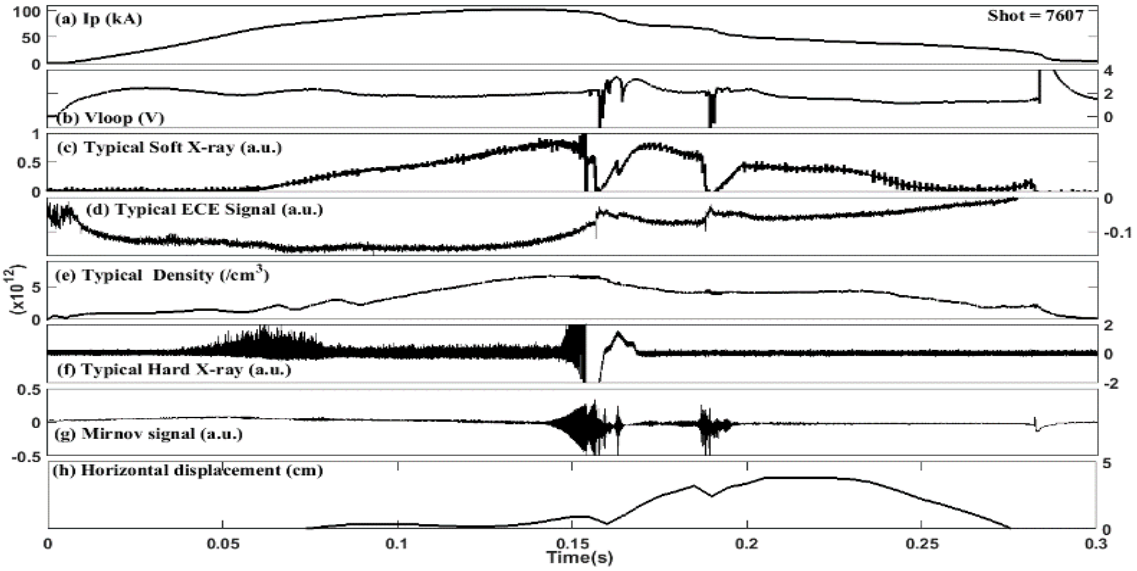

FIG.16. SST-1 shot no. 7607, (a) Plasma current, (b) Loop voltage, (c) Typical Soft X-ray signal, (d) Typical ECE signal, (e) Typical density, (f) Typical Hard X-ray signal, (g) Mirnov signal and, (h) Horizontal displacement

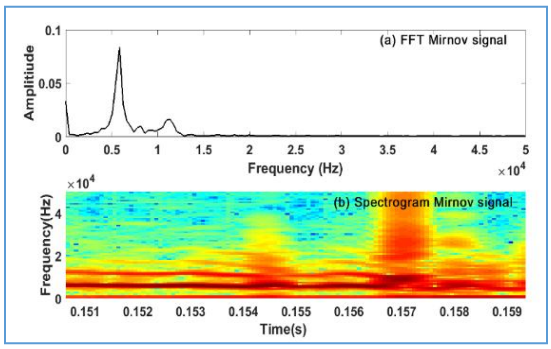

FIG.17. (a) Fourier Transform (b) Spectrogram –Mirnov signal

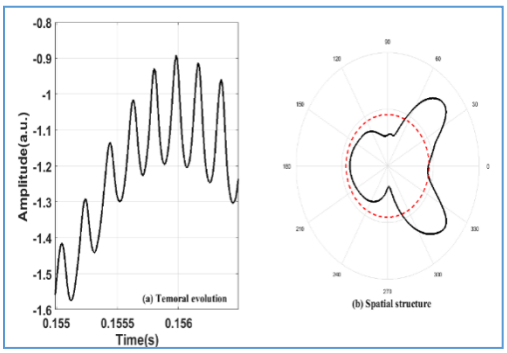

FIG.18. (a) Temporal evolution (b) Spatial structure m=2

4.2. Disruption aspects

Typical discharge with disruption scenario for shot#7606 is shown in Fig.19. The experimentally observed saw teeth period for shot#7607 is ~ 1.4ms. The approximated experimental value of non-linear growth of tearing mode τ_g ~ 0.67ms is nearly half of resistive timescale τ_s = 1.586ms and satisfies the condition $\tau_A < \tau_g < \tau_R$, where ideal time scale τ_A = 0.7μs, resistive diffusion time τ_R = 0.2654s.

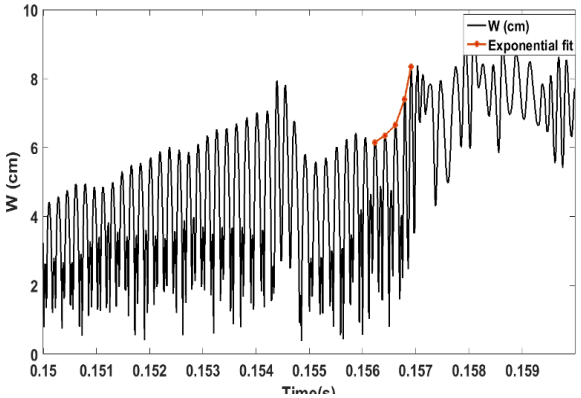

FIG.19. Island width of m=2 mode (black) with exponential fit (red) during interval 156-157ms.

Time evolution of island width (W) during the time interval 150-160ms is shown in Fig. 19. The linear tearing mode growth rate (γ) can be obtained by fitting an exponential function to the time evolution of W [14]. Estimated growth rate γ ~ 450 s^{-1} (Fig. 19) is observed during interval 156-157ms.

We observe m/n=1/1 mode and in later regimes it is accompanied by m/n=2/1 mode with stronger amplitude. Also modulation of m=2 mode by saw teeth oscillations is observed.Mode activity of m/n=2/1 in outer region shows strong activity, grows in amplitude causing few minor disruptions and subsequently large enough to cause major disruption. Disruption scenario (Fig.20) observed suggests radial displacement due to inadequate radial position control as an initiating or precursor event for disruption. The disruptions in large aspect ratio SST-1 plasma seem to depend upon q_a and other main plasma parameters, and suggests them happening not because of density limits.

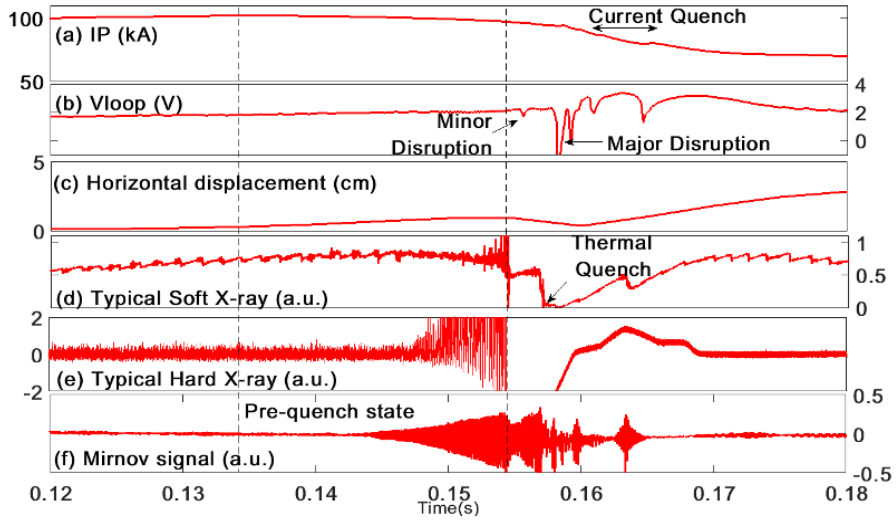

FIG.20. Disruption scenario for shot no. 7607 with Pre cursor, thermal quench and current quench

4.3. Observed Edge Turbulence:

The magnetic and electrostatic fluctuations mainly drive the magnetic and electrostatic turbulence at the tokamak edge [15, 16] and have been investigated in SST-1 over a large number of repeatable shots under identical plasma conditions.

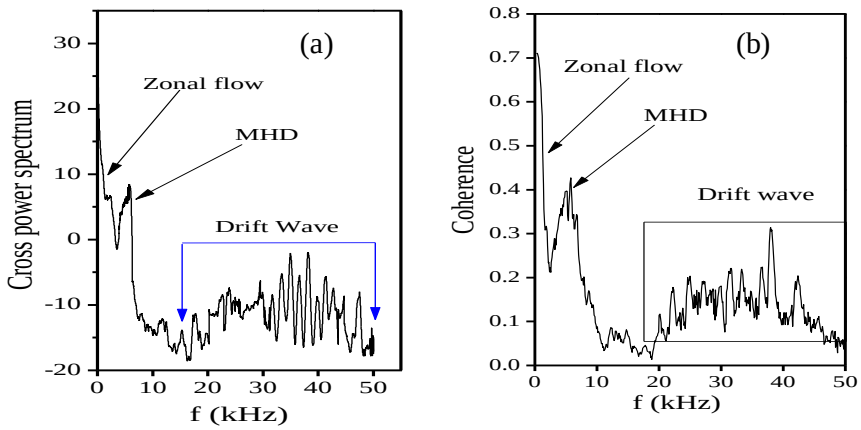

FIG. 21.(a) Cross power spectrum and (b) coherence spectrum for shot no 7799

The cross power spectrum and coherence spectrum of the two signals measured poloidally apart are depicted in Fig. 21 (a) and 21 (b) for shot no 7799. They indicate distinct Zonal flow, MHD and drift waves being present in typical SST-1 plasma. These experimental observations show electrostatic turbulence being modulated by Mirnov oscillations. The high MHD activity synchronizes with the electrostatic fluctuation during SST-1 plasma discharges. Some large-scale coherent structures have also been observed indicating long-distance cross correlation in the poloidal direction.

4.4. Radial and poloidal particle transport at the edge of SST-1

Turbulence driven anomalous transports have been attempted to be experimentally estimated in SST-1 plasma.The radial profile of floating potential fluctuations, ion saturation current fluctuations, electric field fluctuations have been studied at the plasma edge region of SST-1 employing probes. The statistical properties of fluctuation induced radial particle flux at the edge of SST-1 tokamak have been subsequently inferred.

Three similar plasma shots (# 8185, 8205 and 8308) with plasma current reaches in excess of 100 kA have been analysed. The fluctuations in ion saturation current increases from ~15% at r/a = 1.015 to ~20% at r/a = 1.055. i.e. the fluctuations in the ion saturation current decreases in the radially inwards direction. But, almost same fluctuation levels of ion saturation and floating potential are found in poloidal direction at the edge of SST-1 tokamak. The time trace of $\tilde{E}_r = \left(\tilde{V}_{r1} - \tilde{V}_{r2}\right)/d_2$ is measured at the edge of SST-1 tokamak during the MHD activity which is shown in Fig. 22. The radial electric field is presented in normalized form $\left(\tilde{E}_r / \langle E_r \rangle\right)$ with respect to mean radial field. The MHD oscillations appear at t = 160 ms and it exists up to t = 180 ms during the plasma discharge.In the beginning of the magnetic island evolution, a negative radial electric field is found. However, as the magnetic island grows the radial electric field changes from negative to positive. At the end of the MHD activity, again the radial electric field changes slowly from positive to negative value.

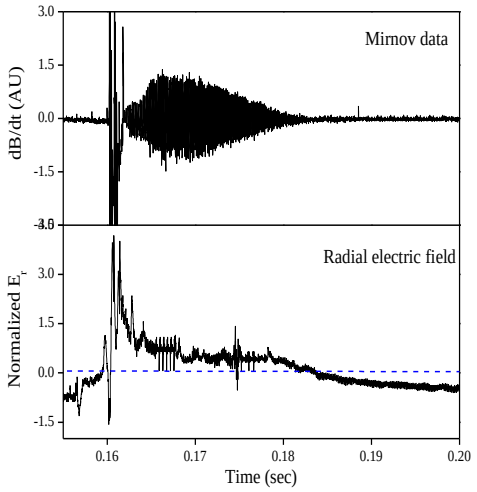

FIG 22: *Mirnov oscillation and radial electric field during plasma discharge.*

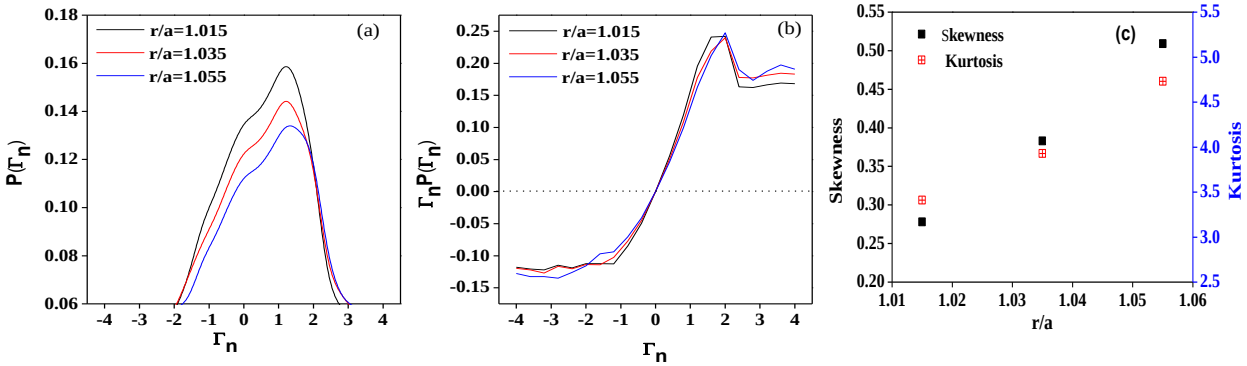

FIG. 23. (a) The local flux PDF, (b) the corresponding flux fraction function at different radial locations and (c) skewness(s) and kurtosis (k) of the PDF

The local flux PDF at different radial locations and the corresponding flux fraction function has been shown in Fig. 23(a) and (b). The PDF shows a clear non-Gaussian character i.e. the local flux PDF is not symmetric. It is seen that the PDF is skewed negatively. The skewness(s) and kurtosis (k) of the PDF have been estimated to non- Gaussian (S = 0, K = 3) distribution. Radially outward, the measured skewness and kurtosis (shown in Fig. 23(c)) values are closure to the expected values for a Bramwell, Holdsworth, and Pinton (BHP) (S = 0.89, K = 4.415) distribution.

5. Future Plans

SST-1 presently aims at implementing several controls in the current profile through an in-house developed control system within the prevailing hardware constraints. The near future plans include plasma current flat-top elongation, extending the plasma duration assisted with LHCD as well as integrating a MW level Neutral Beam Injection system to SST-1.

6. Summary

SST-1 has been upgraded with graphite first wall and is now a compatible Tokamak towards long pulse plasma in both circular and elongated cross sections. Initial experiments have begun in SST-1. Plasma currents in excess of 100 kA with typical core density ~ 1×10^{19} m^{-3} and core electron temperatures ~ 200-300 eV having duration in excess of 300 ms corresponding to q_{edge} ~ 2.6 have been obtained. The pre-ionization induced break down, eddy current induced NULL dynamics, subsequent plasma start-up, copious MHD activities, mode locking and other signatures of standard Tokamak plasma have been obtained. The circular equilibriums have been reconstructed from experimental signals and have been validated with imaging measurements.

SST-1 experiments observe the MHD instabilities such as saw teeth, m/n = 1/1 and m/n = 2/1 tearing modes, similar to the observations reported by other tokamaks. Study of such MHD instabilities and disruption characteristics will be useful for the subsequent disruption mitigation and avoidance strategies in long pulses of SST-1.

Recent experimental results also show that the electrostatic turbulence is modulated by MHD activity during SST-1 tokamak discharge. Some large-scale coherent structures have been observed indicating the long-distance cross correlation in the poloidal direction.

References

[1] S. Pradhan, Z. Khan, V.L. Tanna, et. al , Nuclear Fusion (2015) 55 104009.
[2] D. C. Raval, Z. Khan, Y. Paravastu, et.al, 'Plasma Facing Components Technologies in SST-1', (Poster EX/P5-33 submitted – Fusion Energy Conference 2016, Kyoto, Japan).
[3] S. Jana , S Pradhan, et. al , Fusion engineering and design (Accepted 2016).
[4] D. A. Gates, J. E. Menard,et. al , Review of scientific instruments (2004), 75(12) 5090.
[5] J. A. Leuer et al., Fusion science and technology (2010), 38(3) 333.
[6] S. Jana, S. Pradhan, et al, "Magnetic flux surfaces and Radial Shafranov shifts in SST-1 Tokamak Plasma." (Submitted to Fusion Engineering and Design, 2016).
[7] L. S. Solovev et al, Soviet Physics JETP (1968), 26(2) 400.
[8] V. S. Mukhovatav and Shafranov V D, Plasma equilibrium in a tokamak, Nuclear Fusion (1971), 11 605.
[9] A. SalarElahi and M. Ghoranneviss, Journal of Nuclear and Particle Physics (2012), 2(6)142.
[10] A. Rahimirad, M. Emami et al., Journal of Fusion Energy (2010), 29 73.
[11] J. Dhongde, M. Bhandarkar, et.al, 'MHD Phenomena and Disruption Characteristics in SST-1 Early Plasma', (Poster EX/P5-30 submitted – Fusion Energy Conference 2016, Kyoto, Japan).
[12] J Dhongde, M Bhandarkar, et al., Fusion Engineering Design (2016) 108 77.
[13] J Dhongde, S Pradhan, et al. "MHD mode evolutions prior to minor and major disruptions in SST-1 plasma", (Submitted to Fusion Engineering and Design, 2016).
[14] Pravesh Dhyani, J. Ghosh et al. Nuclear Fusion (2014) 54 083023.
[15] S. Mazur S, P. Nordlund et al., Nuclear Fusion (1994), 34 427.
[16] P. R. Brunsell, Y. Maejima et al., Physics of Plasmas (1994), 1 2297.